ORIGINAL PAPER

Kinetics of Surfactant-induced Aggregation of Lysozyme Studied by Fluorescence Spectroscopy

Neha Jain · Mily Bhattacharya · Samrat Mukhopadhyay

Abstract The study of protein conformational changes in the presence of surfactants and lipids is important in the context of protein folding and misfolding. In the present study, we have investigated the mechanism of the protein conformational change coupled with aggregation leading to size growth of Hen Egg White Lysozyme (HEWL) in the presence of an anionic detergent such as sodium dodecyl sulphate (SDS) in alkaline pH. We have utilized intrinsic protein fluorescence (tryptophan) and extrinsic fluorescent reporters such as 8-anilinonaphthalene-1-sulfonic acid (ANS), dansyl and fluorescein to follow the protein conformational change in real-time. By analyzing the kinetics of fluorescence intensity and anisotropy of multiple fluorescent reporters, we have been able to delineate the mechanism of surfactant-induced aggregation of lysozyme. The kinetic parameters reveal that aggregation proceeds with an initial fast-phase (conformational change) followed by a slow-phase (self-assembly). Our results indicate that SDS, below critical micelle concentration, induces conformational expansion that triggers the aggregation process at a micromolar protein concentration range.

Keywords Fluorescence spectroscopy · Fluorescence anisotropy · Protein aggregation · Lysozyme

Introduction

Protein aggregation refers to abnormal self-association of protein molecules and is implicated in a range of fatal neurodegenerative diseases like Parkinson's and Alzheimer's, systemic amyloidosis etc. [1–3]. Partial unfolding of protein results in the formation of certain critical intermediates which may rearrange by themselves to form oligomeric aggregates that are finally transformed into ordered amyloid fibrils [4]. The striking feature of all the proteins involved in aggregate formation is that they share certain common oligomeric structure and mechanism of toxicity [5]. Studies have been conducted to gain insights into the mechanism of formation of soluble oligomers of various proteins under various *in vitro* solution conditions like high temperature and low pH [6], agitation [7] and pressure [8]. It has been suggested that the critical and oligomeric intermediates formed during fibril formation are more cytotoxic than matured amyloid fibrils [9]. Therefore, it is necessary to unravel the kinetics of protein aggregation to understand how the protein conformational change is coupled with the growth of aggregate size during aggregation. Highly sensitive time-dependent techniques are required to study aggregation to interrogate the intermediates and to illuminate the mechanistic pathway of protein aggregation. Many techniques have been employed to study and characterize aggregation [10], among these fluorescence spectroscopy is an attractive tool [11, 12] that has been utilized to study aggregation of a few model proteins like lactoferrin [13], β_2-microglobulin [14], insulin [15], islet amyloid polypeptide [16] and barstar [17]. The major advantages of fluorescence-based methods in protein aggregation kinetic studies are as follows: (i) Fluorescence observables are very sensitive, and therefore, it is possible to monitor initiation of the aggregation process at a very low protein concentration (ii) Depending on the probe location, fluorescence can report both local and global structural change in proteins (iii) Fluorescence offers a very useful window to probe both conformational change (fluorescence intensity) and size growth (fluorescence polarization/anisot-

N. Jain · M. Bhattacharya · S. Mukhopadhyay (✉)
Indian Institute of Science Education and Research (IISER),
Mohali. Sector 81, S.A.S Nagar,
Mohali 160062 Punjab, India
e-mail: mukhopadhyay@iisermohali.ac.in

ropy) during the protein conformational change driven aggregation process.

Hen Egg White Lysozyme (HEWL) is an archetypal protein which has been extensively used to understand the mechanism of protein folding, misfolding and amyloid formation [18–21]. It is an attractive protein to use as a model because (i) it is a small single-domain protein with 129 amino acids and molecular weight of 14.6 kDa (ii) it contains diverse secondary structural elements such as α-helix, β-sheet and random coil (Fig. 1) and (iii) it has a high degree of sequence and structural homology with human lysozyme that has been implicated in human amyloidosis [22, 23]. Lysozyme forms fibrils under different conditions like high temperature and low pH [24], mutations [25], proteolytic cleavage [26] and chemical modification [27]. It has been reported that aggregates of HEWL are toxic to cell cultures [28, 29]. Aggregation of HEWL is shown to be a nucleation-dependent phenomenon which gives rise to a lag-phase and an assembly phase [30]. Lysozyme also interacts with surfactants [31, 32] and denaturants [33] to form amyloid fibrils under carefully-controlled *in vitro* conditions. The most commonly used surfactant is sodium dodecyl sulfate (SDS) which is an anionic detergent and mimics many features of biological membranes. SDS can bind to a variety of proteins and depending on its concentration, it may either induce or inhibit the aggregation [34, 35]. The lysozyme-SDS complex has been studied in the context of biopolymer-

surfactant interaction [36, 37]. At pH lower than isoelectric point (pI 11), SDS interacts with positively charged exterior surface of HEWL and causes turbidity which is reduced with an increase in pH [38]. It was also shown that HEWL behaves differently in the presence of SDS at pH 9.2, where it leads to the formation of amyloid-like fibrils [31].

The mechanism of the interaction of HEWL with SDS leading to oligomerization and aggregate formation is poorly understood. In the present investigation, we aimed at probing the mechanism of early conformational- and size changes during the course of aggregation in HEWL at pH 9.2 in the presence of SDS using fluorescence spectroscopy. We have utilized various reporters to shed light into the aggregation mechanism. Steady-state fluorescence intensity and anisotropy of different fluorescent reporters were used to extract information about the protein conformational change and the overall size growth that lead to the formation of soluble aggregates. The kinetic parameters recovered from the fluorescence kinetics have been used to suggest a mechanistic model of surfactant-induced aggregation of lysozyme.

Materials and Methods

Materials

Hen Egg White Lysozyme (HEWL), 8-anilinonaphthalene-1-sulfonic acid ammonium salt (ANS) and Fluorescein-5-

Fig. 1 **a** Structure of Hen Egg White Lysozyme (HEWL; protein data bank ID: 1GWD; drawn using PyMol) showing tryptophans (*red*) and disulfide bonds (*green*) **b** Distribution of surface charge on HEWL (positive: *blue* and negative: *red*) **c** The amino acid sequence of HEWL

```
1                                                  50
KVFGRCELAAAMKRHGLDNYRGYSLGNWVCAAKFESNFNTQATNRNTDGS
51                                                 100
TDYGILQINSRWWCNDGRTPGSRNLCNIPCSALLSSDITASVNCAKKIVS
101                          129
DGNGMNAWVAWRNRCKGTDVQAWIRGCRL
```
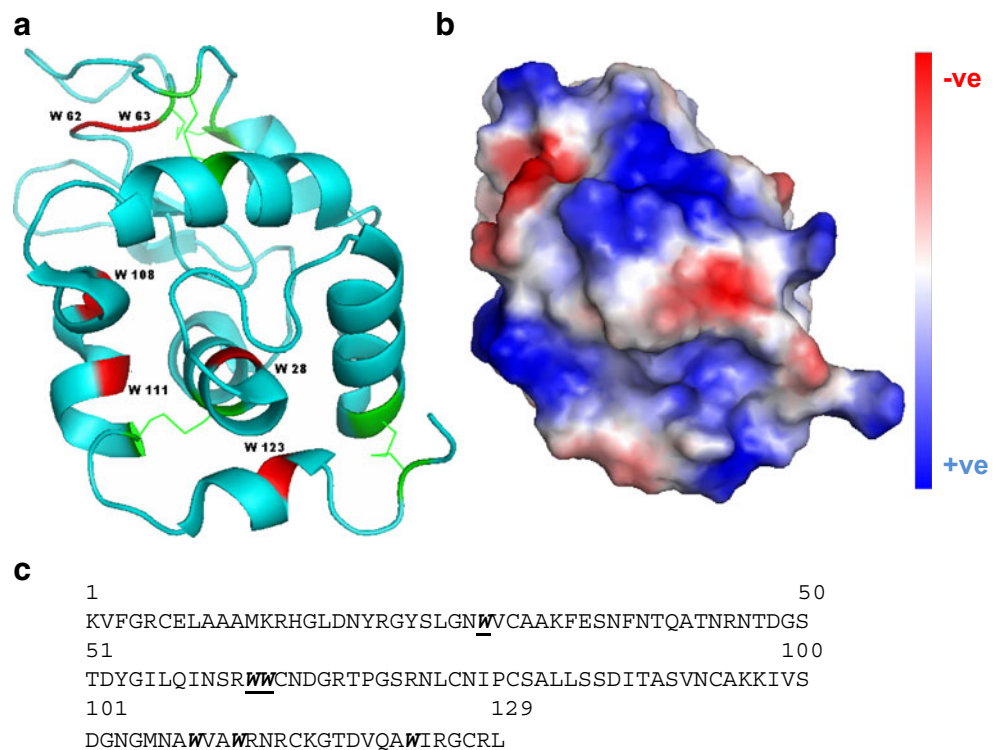
Figure 1

(6)-isothiocyanate (FITC) were purchased from Sigma-Aldrich. 5-Dimethylaminonaphthalene-1-sulfonyl chloride (Dansyl Chloride) was obtained from Molecular Probes (Invitrogen). All other chemicals were of analytical grade and were used as received.

Sample Preparation

HEWL with a concentration of 1 mM was prepared in Milli-Q water and stored at 4 °C. Protein concentration was determined by measuring the absorbance at 280 nm using Perkin Elmer Lambda 25 UV-Vis Spectrophotometer. The extinction coefficient of HEWL is 38,000 $M^{-1}cm^{-1}$ [39]. For all the experiments, a final concentration of 5 μM HEWL was used except for concentration dependence studies, where it ranged from 1 μM to 5 μM. Buffers with stock of 500 mM were prepared in Milli-Q water: Sodium Phosphate (pH 7–8) and Glycine-NaOH (pH 9, 9.2, and 10) and stored at 4 °C. Buffers were diluted 10-fold to yield a final concentration of 50 mM. pH of each buffer was adjusted using Cyberscan 510 pH meter procured from Eutech Pvt. Ltd with an accuracy of ±0.02. A stock of 100 mM Sodium Dodecyl Sulphate (SDS) was prepared in Milli-Q water. SDS was stored at room temperature (~ 24 °C). FITC solution was prepared in DMSO (dimethyl sulfoxide) and Dansyl chloride solution was prepared in DMF (dimethyl formamide) with a concentration of 5 mM. All probes were freshly dissolved in the required solvent and used in the labeling reaction immediately.

Fluorescence Labeling of HEWL with Different Fluorophores

Surface labeling of HEWL was performed with Fluorescein isothiocyanate that reacts with the accessible amino groups of proteins. The procedure recommended by Molecular Probes was followed with slight modifications. Labeling was performed in freshly prepared 0.1 M Na_2CO_3-NaHCO_3$ buffer of pH 9 with equimolar proportions of HEWL and probe. The reaction was stirred on a stirrer in dark for 90 min at room temperature. Once the reaction was over, free dye was removed from labeled protein by transferring it into MICROCON YM 3 (cutoff 3,000 Da; procured from Millipore) and centrifuging at 11,000 rpm. The absorbance of filtrates and concentrated labeled protein were measured as a ratio at 280 nm and 488 nm for FITC labeled HEWL. Finally, the degree of labeling was determined using the molar extinction coefficient of 64,000 $M^{-1}cm^{-1}$ for FITC [40]. The protein was also labeled separately with dansyl chloride which covalently reacts with the amino groups of the surface residues of protein. Equimolar concentration of HEWL and dansyl chloride (500 μM) was taken in 0.1 M Na_2CO_3-NaHCO_3$ buffer (pH 9). The reaction mixture was allowed to stand for 2 h at room temperature in the dark with intermittent mixing. After the reaction was over, it was stored at 4 °C in the dark.

Tryptophan Fluorescence

Perkin Elmer LS 55 spectrofluorimeter was used to record steady-state fluorescence in a cuvette having pathlength of 10 mm. Following parameters were adjusted to monitor tryptophan intensity during aggregation: λ_{ex}=280 nm with an excitation bandpass of 2.5 nm; λ_{em}=350 nm with an emission bandpass of 2.5 nm. The kinetic data were collected at an interval of 10 s with an integration time of 5 s. For the equilibrium data, the emission spectra were recorded after 30 min of incubation with a scan speed of 10 nm/min and averaged over five scans. Fluorescence anisotropy $[r=(I_{ll} - I_{\perp}.G)/(I_{ll}+2I_{\perp}.G)]$ was recorded (λ_{ex}= 300 nm, bandpass 2.5 nm; λ_{em}=350 nm, bandpass 9 nm) from the parallel (I_{ll}) and perpendicular ($I_{\perp}$) intensity components with the G-factor correction. For anisotropy measurements, an integration time of 30 s was used to obtain a satisfactory signal-to-noise.

ANS Fluorescence

A stock of 10 mM ANS in Milli-Q water was prepared and stored in the dark at 4 °C. For all the experiments, a 1,000-fold dilution of the stock was used to yield the final concentration of 10 μM ANS. The time-course of the ANS fluorescence intensity was used to characterize the aggregation kinetics. The following parameters were adjusted during the kinetic runs: λ_{ex}=350 nm with an excitation bandpass of 2.5 nm; λ_{em}=475 nm with an emission bandpass of 5 nm. The kinetic data were collected at an interval of 10 s with an integration time of 5 s. For the equilibrium data, the emission spectra were recorded after 30 min of incubation with a scan speed of 10 nm/min and averaged over five scans. The ANS fluorescence anisotropy was monitored with an excitation and emission bandpass of 2.5 nm and 8 nm, respectively with an integration time of 30 s. Perpendicular intensity components were corrected using the G-factor.

Aggregation Conditions

Aggregation reaction with unlabeled protein was initiated by adding 5 μM HEWL to 150 μM SDS at pH 9.2 with a manual mixing deadtime of 10 s and the process was monitored over a period of time. Concentration dependence studies were performed as a function of (i) varying SDS concentration from 25 μM–200 μM (ii) varying HEWL concentration from 1 μM–5 μM. Control experiments were performed at pH 7, 8, 9 and 10 under similar conditions.

All the experiments were carried out at room temperature (24–25 °C).

Aggregation with Fluorescein Labeled Protein

The fluorescein-labeled protein was mixed thoroughly with the unlabeled protein under native non-aggregating condition at pH 7. The labeled protein concentration was 2% of the total protein used in the reaction mixture. A total protein concentration of 5 μM having 100 nM of the labeled protein was used to monitor the changes in the fluorescence intensity and anisotropy upon addition of SDS (150 μM) at pH 9.2. The following parameters were used: λ_{ex}=488 nm with an excitation bandpass of 2.5 nm; λ_{em}=514 nm with an emission bandpass of 4 nm (for intensity) and 7 nm (for anisotropy). The integration time was 5 and 30 s for the measurement of fluorescence intensity and anisotropy, respectively. The error in fluorescence anisotropy was below 0.01.

Aggregation with Dansyl Labeled Protein

The dansyl-labeled protein was mixed thoroughly with the unlabeled protein under native non-aggregating condition at pH 7. The labeled protein concentration was 20% of the total protein used in the reaction mixture. A total protein concentration of 5 μM having 1 μM of the labeled protein was used to monitor the changes in the fluorescence intensity and anisotropy upon addition of SDS (150 μM) at pH 9.2. The following parameters were used: λ_{ex}= 340 nm with an excitation bandpass of 2.5 nm; λ_{em}= 500 nm with an emission bandpass of 5 nm (for intensity) and 8 nm (for anisotropy). The integration time was 5 and 30 s for the measurement of fluorescence intensity and anisotropy, respectively.

Circular Dichroism (CD) Spectroscopy

The far-UV CD spectra of the protein samples were recorded on an Applied PhotoPhysics Chirascan CD spectrometer at room temperature. For the acquisition of CD spectra, the protein sample solutions were taken in a quartz cuvette of 2 mm pathlength and the secondary structural changes were recorded in the range of 190–260 nm. The scan rate was 1 nm/s and the final spectrum was the average of four scans. The spectra were corrected with buffer baseline subtraction and were smoothened using the Chirascan software. For kinetic experiments, HEWL at pH 9.2 was taken in a quartz cuvette of 10 mm pathlength and SDS was added with a manual mixing deadtime of 10 s. The loss of helicity was monitored by ellipticity at 222 nm.

Data Analysis

The data were plotted and analyzed with non-linear curve fitting method using commercially available OriginPro Version 8.0 Software. All the plots were fitted to more than one function and the best fit was used to explain the kinetics of the process. The goodness of the fit was determined by the adjusted R^2 and residual analysis.

Results

Intrinsic and Extrinsic Fluorescence of Lysozyme in the Presence of SDS

The native monomeric form of hen egg white lysozyme (HEWL) converts into insoluble amyloid-like aggregates upon incubation with sodium dodecyl sulfate (SDS) at pH 9.2 at room temperature [31]. Our interest in the mechanism of protein aggregation led us to investigate the early events of the protein conformational change and aggregation that converts the monomeric protein into soluble oligomers. We have used three different fluorescent reporters namely tryptophan (intrinsic fluorophore), ANS (non-covalently bound fluorophore) and dansyl and fluorescein (covalently attached fluorophore) to observe the structural changes of HEWL in the presence of SDS at pH 9.2. Figure 2 shows the fluorescence emission spectra and the steady-state anisotropy plots of different fluorescent reporters in HEWL under different solution conditions at equilibrium. Upon addition of SDS, there was a substantial increase in the tryptophan, ANS and dansyl fluorescence intensity with a concomitant blue shift in the emission wavelength. Since protein aggregation in water is largely driven by hydrophobic interaction of exposed hydrophobic patches, ANS-fluorescence provides a useful readout of the aggregation process. Our results indicate that under the aggregating condition, HEWL may undergo a conformational transition to partially unfolded 'molten globule'-like state comprising hydrophobic binding pockets for ANS. This expanded conformer associates to form oligomeric aggregates as evident from the increase in the steady-state fluorescence anisotropy for all three probes for the protein at pH 9.2 in the presence of SDS. Large fluorescence anisotropy revealed the increase in overall size due to protein aggregation leading to soluble oligomer formation. Upon prolonged incubation, aggregates further grew in size and could be visually seen from the increase in the turbidity. These observations prompted us to devise fluorescence-based kinetic experiments to investigate the mechanism of lysozyme aggregation in the presence of SDS.

Fig. 2 Surfactant-induced changes in **a** fluorescence spectra and **b** anisotropy of different probes (tryptophan, ANS and dansyl) upon addition and incubation of 5 μM HEWL with 150 μM SDS at pH 9.2 at room temperature. All the experiments were repeated separately at least three times and were highly reproducible
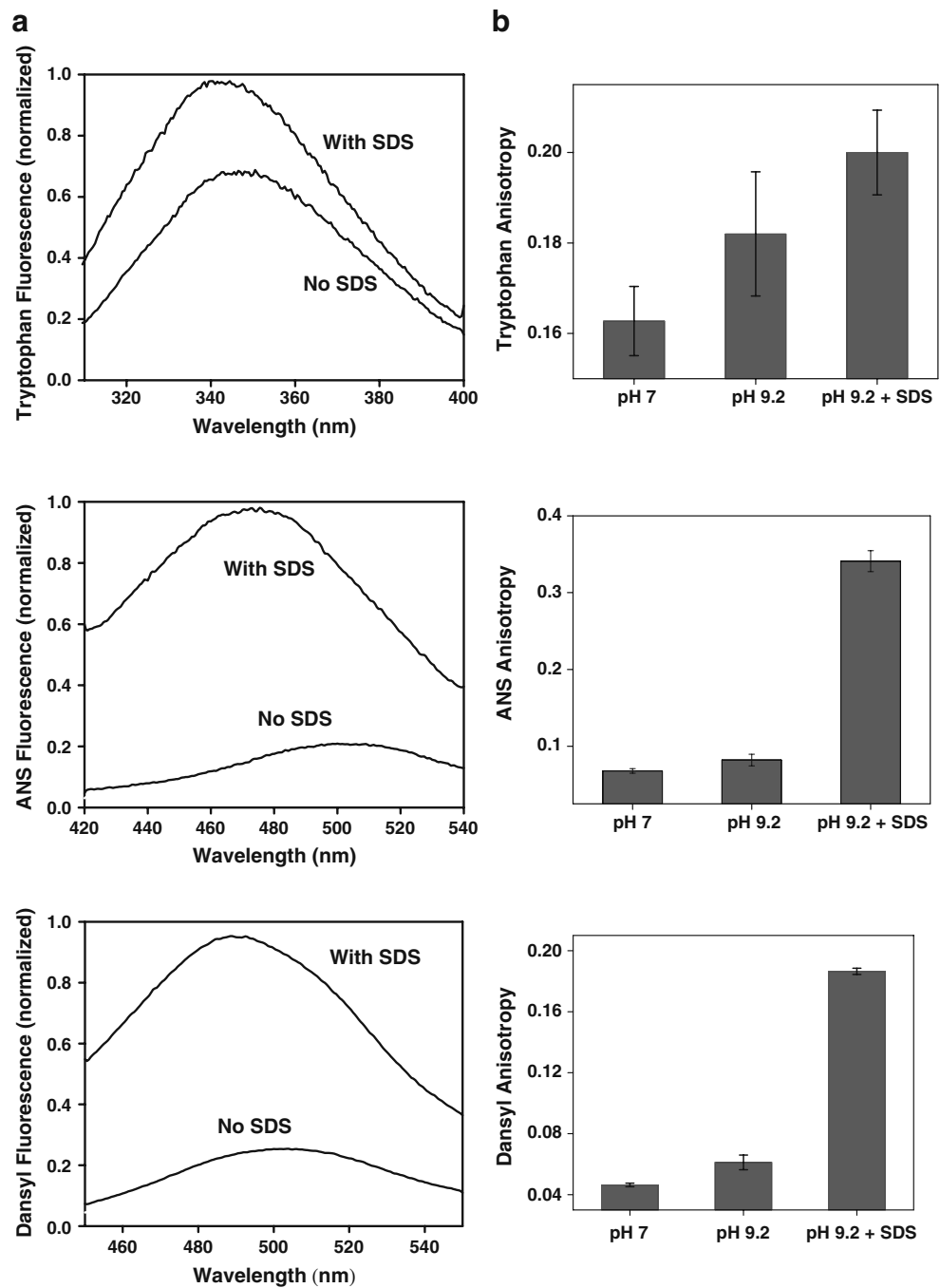

Dependence of pH, Surfactant Concentration and Protein Concentration

In order to ascertain the emergence of hydrophobic regions as a result of conformational changes during the course of HEWL aggregation, we used ANS that is widely used to characterize partially unfolded 'molten-globule' states of the protein [41]. It is an environment-sensitive dye which is weakly fluorescent in aqueous solution but fluoresces strongly when it is non-covalently bound to a hydrophobic microenvironment. ANS has also been used previously as a reporter to probe protein aggregation [42]. In order to investigate whether HEWL aggregation occurs at other pH where negatively charged SDS can interact with positively charged Lysozyme (Fig. 1b), the change in ANS fluorescence intensity in the presence of HEWL and SDS (150 μM) was monitored over a period of time at several pH ranging from the neutral to alkaline (Fig. 3a). In the

Fig. 3 Time-course of ANS fluorescence intensity as a function of HEWL aggregation in presence of SDS with variation in **a** pH, **b** SDS concentration and **c** protein concentration. **d** A triggering experiment is shown with the addition of SDS (final concentration 150 μM). All the experiments were repeated separately at least twice and were highly reproducible
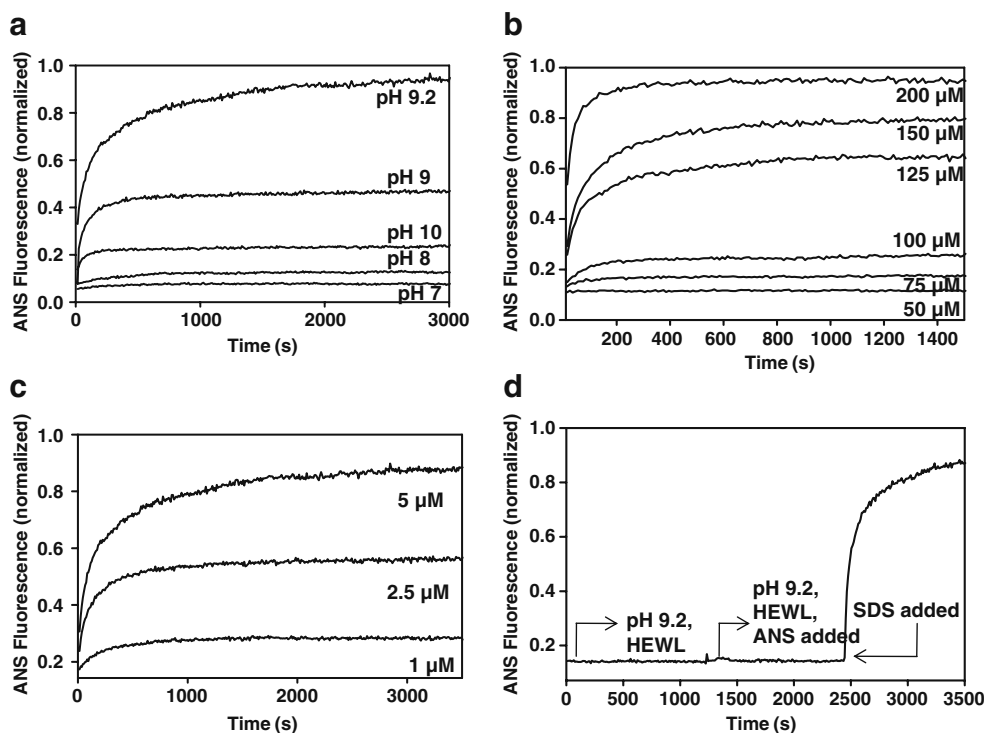
presence of HEWL at pH 9.2, ANS fluorescence was very low. A 10-fold increase in the fluorescence was observed within a few minutes of addition of SDS which reached saturation after 40 min whereas at other pHs (7, 8, 9 and 10) the extent and the rate of increase in the ANS fluorescence was much less significant. To identify the optimal concentration of SDS required for HEWL aggregation, we performed concentration dependent studies whereby the concentration of SDS was varied from 50 μM to 200 μM. Figure 3b shows an increase in the ANS fluorescence intensity with an increase in SDS concentration. At higher SDS concentrations (viz. 500 μM), ANS fluorescence initially increased as observed at lower SDS concentrations and then it decreased. Our further studies were made at the range of SDS concentration from 50 μM to 200 μM. It is worth mentioning here that the concentration of SDS used for the aggregation experiments is significantly lower than its critical micelle concentration (∼ 8 mM) [43]. Additionally, we performed protein concentration dependent studies to identify the optimal concentration of HEWL for aggregation since protein concentration plays a crucial role in the aggregation processes. In this set of experiments, ANS fluorescence intensity was monitored at various HEWL concentrations (from 1–5 μM) in the presence of 150 μM SDS at pH 9.2 (Fig. 3c). At higher protein concentrations, the solutions turned turbid immediately and therefore, reliable fluorescence measurements could not be performed. Therefore, the optimal condition for aggregation experiments was set at 150 μM of SDS with 5 μM of HEWL at pH 9.2. To

confirm the decisive role of SDS in protein aggregation further, a triggering experiment (Fig. 3d) was performed in which no detectable fluorescence intensity was observed for HEWL at pH 9.2 without ANS (initial part of Fig. 3d) and with ANS (second part of Fig. 3d). These observations indicate that there is no hydrophobic pocket available in the monomeric HEWL to which ANS can bind. Then the aggregation was triggered by adding a stock solution of SDS (final trace in Fig. 3d). As soon as SDS was added and mixed to the protein solution, there was a time-dependent increase in the ANS fluorescence suggesting the formation of aggregates containing hydrophobic-rich regions to which ANS can bind. This set of experiments convincingly demonstrated that the protein molecules aggregate at pH 9.2 which is mediated by negatively-charged SDS. Control experiments showed that in the absence of HEWL, the ANS fluorescence was negligible at all the SDS concentrations used for the present study, thus, emphasizing the fact that upon interaction with SDS, HEWL association occurs which leads to the formation of aggregates driven by hydrophobic association of conformationally altered HEWL.

To investigate whether the negative charge on the SDS molecules plays a crucial role in HEWL aggregation, we performed similar experiments with cationic surfactants such as, cetyl tetramethylammonium bromide (CTAB). ANS-binding experiments revealed that CTAB did not facilitate protein aggregation at pH 9.2 (data not shown) which indicated that the negatively charged SDS indeed promotes HEWL aggregation at pH 9.2. Interestingly,

anionic bile salt surfactants (sodium cholate and sodium deoxycholate) did not induce aggregation under identical conditions. Next, we investigated the kinetics of a number of fluorescence observables under identical aggregation condition to shed light into the mechanism of surfactant-induced lysozyme aggregation.

Kinetic Analysis of Lysozyme Aggregation Using Multiple Fluorescent Reporters

First, we carried out kinetic experiments with ANS to monitor the protein conformational change leading to a partially unfolded 'molten globule'-like state that associates to form oligomers. In the presence of 10 μM ANS, HEWL was mixed with SDS at pH 9.2 using manual mixing with a deadtime of 10 s. The time-dependence of ANS fluorescence intensity exhibited a sharp rise during the aggregation process. A single exponential kinetics was inadequate to describe the processes as revealed by a considerable misfit (Fig. 4a). A double exponential kinetics was able to satisfactorily describe the time-dependent changes in the fluorescence intensity (Fig. 4b). In all the experiments, the

absence of a lag phase was observed. The increase in ANS fluorescence was fitted to a double exponential function which suggests that the aggregation is a biphasic process where a rapid-initial phase is followed by a slow phase (Fig. 5a). The recovered rate constants obtained from the ANS fluorescence kinetics were $k_{fast} \sim 12 \times 10^{-3}$ s^{-1} and $k_{slow} \sim 1.2 \times 10^{-3}$ s^{-1}. This may suggest that upon addition of SDS, HEWL undergoes a fast conformational transition to a partially unfolded 'molten-globule'-like state that eventually associates to form soluble aggregates in slower kinetics. The decrease in the secondary structural contents during the time-course was also evident by the loss of helicity from the circular dichroism spectroscopy (Fig. 4c–d). Next, we performed the kinetic experiments by monitoring the intrinsic tryptophan fluorescence as a function of aggregation.

Tryptophan is an intrinsic fluorophore whose emission maximum depends on the polarity of its microenvironment. The emission maximum of tryptophan, when exposed to an aqueous medium, is ~350 nm whereas it exhibits a blue-shift when buried inside a hydrophobic environment [11]. As mentioned earlier, at pH 9.2 and in the presence of SDS, an increase in the tryptophan fluorescence intensity was

Fig. 4 Comparison between **a** single and **b** double exponential fit for ANS-fluorescence kinetics during aggregation of HEWL (5 μM) in presence of SDS (150 μM) at pH 9.2. Residual plots obtained for the respective fits are also shown. **c** CD spectra of HEWL at pH 9.2 in the absence of SDS (i), 5 min (ii), 15 min (iii) and 45 min (iv) after adding SDS (150 μM). **d** Kinetics of the loss of helicity probed by CD at 222 nm during aggregation of HEWL (5 μM) in the presence of SDS (150 μM) at pH 9.2. The double exponential fit is shown in *solid line*
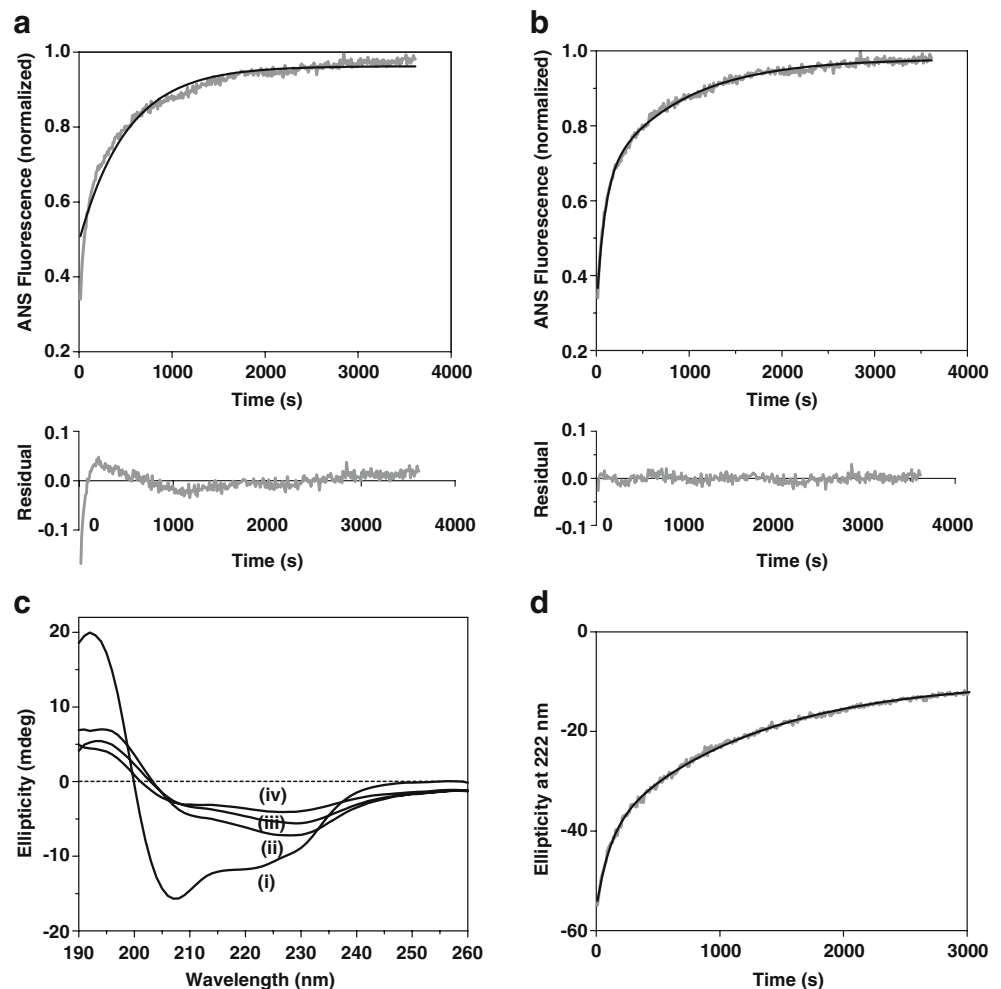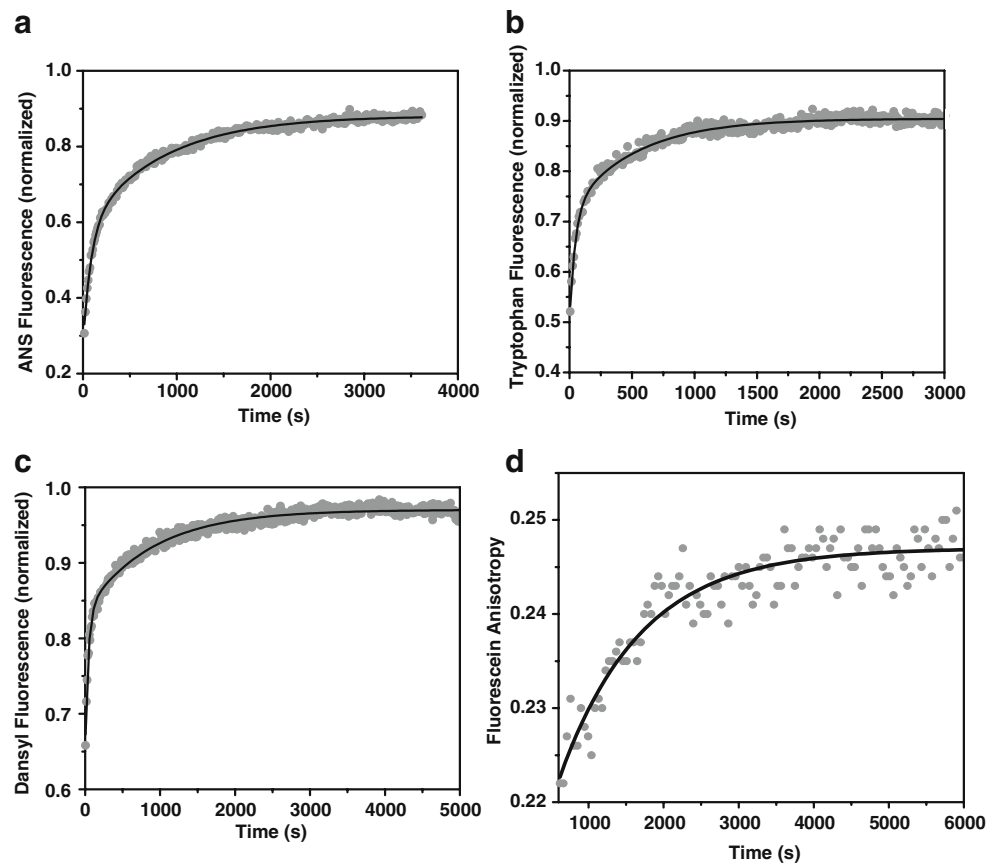
Fig. 5 Time-course of aggregation of HEWL at pH 9.2 in presence of SDS (150 μM) studied with multiple fluorescent reporters in-tandem: **a** ANS Fluorescence **b** Tryptophan Fluorescence **c** Dansyl Fluorescence in dansyl labeled HEWL and **d** Fluorescence anisotropy of fluorescein labeled HEWL. Fits are shown in *solid lines*

observed with a concomitant blue-shift to ~340 nm with a simultaneous increase in the fluorescence anisotropy. Both the observations suggest that the aggregation of HEWL occurs in the presence of SDS whereby the tryptophans get buried inside the hydrophobic interior formed upon association. This prompted us to probe into the time-dependent changes in the tryptophan fluorescence as a function of aggregation. A sharp rise in the tryptophan fluorescence was observed which reached a quasi-plateau within 15 min and then attained saturation (Fig. 5b). Here again, a double exponential kinetics was able to describe the time-dependent changes in the tryptophan fluorescence indicating a fast and a relatively slower kinetic components. The observed rate constants for the changes in tryptophan fluorescence intensity were found to be $k_{fast} \sim 22 \times 10^{-3}$ s^{-1} and $k_{slow} \sim 2 \times 10^{-3}$ s^{-1}. The initial, rapid phase may indicate the protein conformational changes to extended conformers whereas the slower phase could be ascribed to the aggregation process. HEWL contains six tryptophan residues (Fig. 1c) among which Trp 63 and 123 are non-fluorescent due to the proximity of the tryptophans with the sulfur atoms of the disulfides [19, 20, 44]. The initial increase in the tryptophan fluorescence (k_{fast}) is interpreted as protein conformational expansion that diminishes the quenching of non-fluorescent tryptophan residues by the disulfides. The increase in the tryptophan fluorescence in

the latter phase (k_{slow}) arises due to burial of the tryptophan residues into the hydrophobic core of the aggregates.

Comparison of the fast component of the rate constants obtained for the change in tryptophan and ANS fluorescence reveals that the rate of change in tryptophan fluorescence kinetics is ~2-fold faster than the ANS fluorescence kinetics.

To further investigate the mechanism of aggregation, we labeled the protein surface sparsely with different fluorophores and monitored the changes in fluorescence properties during aggregation under identical condition. The protein was labeled with dansyl chloride (for details, see Materials and Methods) and the aggregation was monitored by dansyl fluorescence. A rapid increase in dansyl fluorescence intensity, similar to that of tryptophan and ANS, was observed (Fig. 5c). A double exponential function was again required to fit the kinetics of dansyl fluorescence data. The recovered rate constants were $k_{fast} \sim 24 \times 10^{-3}$ s^{-1} and $k_{slow} \sim 1 \times 10^{-3}$ s^{-1}. It is interesting to note that the fast component of rate constant of the dansyl fluorescence is similar to that of tryptophan and both tryptophan and dansyl fluorescence readouts probe the conformational change of the polypeptide chain. Next, we carried out the fluorescence anisotropy kinetics to follow the size growth of the oligomers during aggregation.

In order to obtain the steady-state fluorescence anisotropy as a function of HEWL aggregation, we labeled the protein
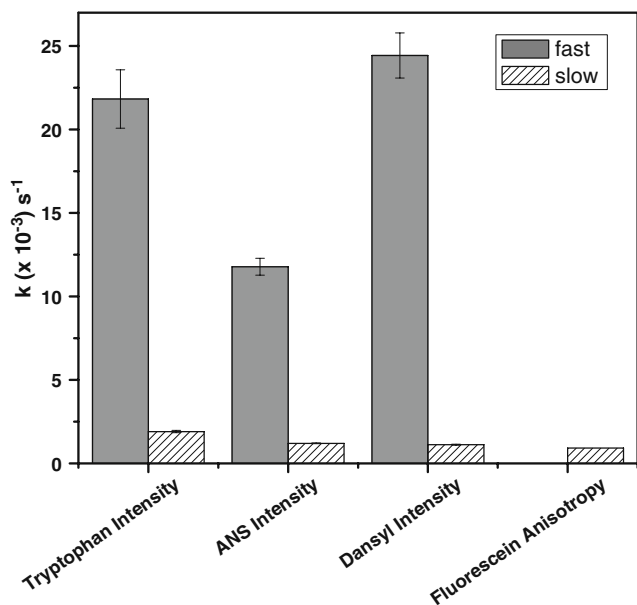
Fig. 6 Fast and slow components of the apparent rate constants of different fluorescent reporters during the aggregation process

surface sparsely with another surface-modifying fluorophore, namely, fluorescein isothiocyanate. The reason for choosing fluorescein was that its fluorescence property is largely environmental insensitive [11], and therefore, the change in the steady-state fluorescence anisotropy is primarily dominated by the change in the overall rotational correlation time. The steady-state fluorescence anisotropy showed a steady increase that could be satisfactorily described by single exponential kinetics and the recovered rate constant ($\sim 1 \times 10^{-3}$ s^{-1}, Fig. 5d.) is similar to the slower kinetic component (k_{slow}) obtained from the kinetics of ANS, tryptophan and dansyl fluorescence. This also indicates that the slower kinetic component (k_{slow}) in other fluorescence observables represents the aggregate growth.

As it has been discussed, we can infer that under the present set of experimental conditions, lysozyme aggregation is at least a two-step process as described by the double exponential fitting analysis. Figure 6 depicts a comparison
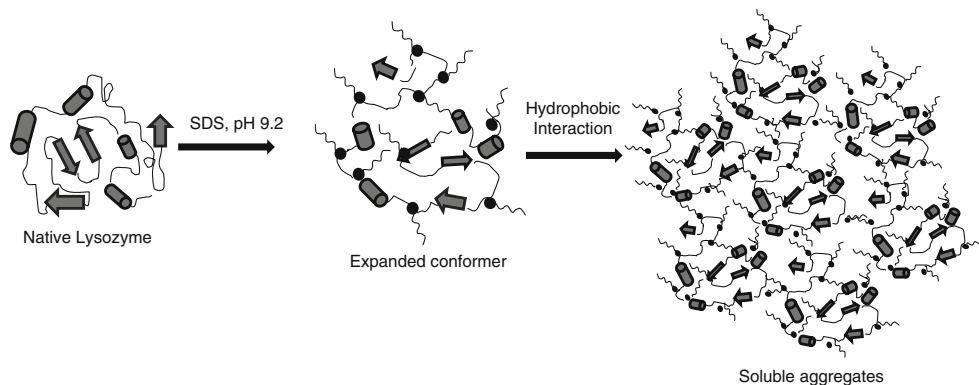
between the recovered rate constants with standard deviations obtained from the analysis. The rates of change in tryptophan ($k_{fast} \sim 22 \times 10^{-3}$ s^{-1}) and dansyl fluorescence intensities ($k_{fast} \sim 24 \times 10^{-3}$ s^{-1}) are similar and faster than the rate constants extracted for ANS intensity ($k_{fast} \sim 12 \times 10^{-3}$ s^{-1}). Such a comparison reflects that the fluorophores report two distinct aspects of aggregation. As tryptophan is more sensitive to its environment, it reports any change that affects the lysozyme native conformation whereas, ANS reports the generation of hydrophobic sites as a consequence of conformational change and oligomerization. Fluorescence anisotropy showed a single component which resembles with the slower components of other observables demonstrating the aggregation process.

Discussion

Protein aggregation occurs through various mechanisms and different methods have been used to delineate the process [45]. In the present study, we have investigated the conformational and size change during aggregation of HEWL in the presence of SDS at alkaline pH. We have used a variety of fluorescent markers to get insights into the mechanism of aggregation. A sharp increase in the fluorescence properties of all the probes under prevailing conditions indicate the protein conformational change coupled with aggregation of HEWL. In the native protein and in the absence of SDS, these probes are either exposed to the solvent or to certain residues which may quench their fluorescence. Also, the probes have high degree of rotational motion and thus contribute to low fluorescence anisotropy. Upon addition of SDS at pH 9.2, conformational change in the HEWL brings them in an environment where they exhibit high fluorescence intensity and the overall rotational motion is restricted due to an increase in the overall size as a result of aggregation, thus, giving high fluorescence anisotropy. We suggest that SDS being negatively charged interacts electrostatically with positively charged surface of lysozyme (Fig. 1b) at pH 9.2 (pI$\sim$11).

Fig. 7 A proposed model for SDS-induced aggregation of lysozyme

This interaction neutralizes surface charge on the protein and increases hydrophobicity which is in accordance with a previous study where similar mode of interaction was observed by the formation of SDS-lysozyme complex [36]. Reduction of overall protein charge facilitates penetration of negatively charged SDS into the protein-core leading to the conformational change resulting in the formation of extended conformers. It was also noticed that by changing the non-polar linear, alkyl chain of SDS to a cyclic, fused ring system such as, sodium cholate and sodium deoxycholate did not foster the formation of HEWL aggregates. We speculate that in addition to the negative charge on the head group, the linear hydrocarbon tail might play an important role in stabilizing the surfactant-protein interaction, thus favoring the conformational expansion of the lysozyme. Such conformational change may facilitate intermolecular interactions driven by hydrophobic effects and eventually lead to the aggregation of protein molecules [31]. The remarkable feature of this aggregation is that it requires protein and SDS in very low concentrations viz. 5 μM and 150 μM, respectively. This is in contrast to most of the studies where a high concentration of protein is required for protein aggregation [32, 33].

An increase in ANS fluorescence intensity during aggregation reflects that the conformational expansion due to SDS-lysozyme interaction creates some hydrophobic pockets to which ANS can bind non-covalently and the number of hydrophobic sites increases to a certain extent as aggregation progresses. However, the initial increase in ANS intensity is slower than that of tryptophan, suggesting that formation of hydrophobic regions and hence oligomerization, occurs as a consequence of the conformational change of the polypeptide chain. The overall increase in the fluorescence anisotropy of different probes also indicates that the conformational change in the protein facilitates association of protein molecules which restricts the rotational motion of the fluorophore, thus exhibiting large fluorescence anisotropy. The overall finding of this study involves an understanding of lysozyme aggregation in the presence of an anionic surfactant. A plausible mechanism of HEWL aggregation can be suggested based on our observations (Fig. 7). Initially, the protein interacts with SDS by virtue of electrostatic interaction that leads to a conformational expansion in the protein. This in turn, directs the formation of oligomers mediated by hydrophobic interactions that subsequently lead to the formation of lysozyme aggregates.

Conclusions

In the present study, we have attempted to understand the basic mechanism of aggregation by providing insights into the change in protein conformation and size using fluorescence spectroscopy. It is important to mention that the protein concentrations used in our experiments are significantly lower than that in typical aggregation experiments which are often carried out at the millimolar protein concentration range. This type of surfactant-protein interaction may be relevant in certain critical interactions between lipid membrane and proteins inside the cell leading to aggregation. We believe that our fluorescence kinetics analysis will find broad application in the area of protein misfolding and aggregation.

References

1. Luheshi LM, Crowther DC, Dobson CM (2008) Protein misfolding and disease: from the test tube to the organism. Curr Opin Chem Biol 12:25–31
2. Soto C (2003) Unfolding the role of protein misfolding in neurodegenerative diseases. Nat Rev Neurosci 4:49–60
3. Pepys MB, Hawkins PN, Booth DR, Vigushin DM, Tennent GA, Soutar AK, Totty N, Nguyen O, Blake CCF, Terry CJ, Feest TG, Zalin AM, Hsuan JJ (1993) Human Lysozyme gene mutation cause hereditary amyloidosis. Nature 362:553–557
4. Uversky VN, Fink AL (2004) Conformational constraints for amyloid fibrillation: the importance of being unfolded. Biochim Biophys Acta 1698:131–153
5. Kayed R, Head E, Thompson JL, McIntire TM, Milton SC, Cotman CW, Glabe CG (2003) Common structure of soluble amyloid oligomers implies common mechanism of pathogenesis. Science 300:486–489
6. Kumar S, Mohanty SK, Udgaonkar JB (2007) Mechanism of formation of amyloid protofibrils of barstar from soluble oligomers: evidence for multiple steps and lateral association coupled to conformational conversion. J Mol Biol 367:1186–1204
7. Sluzky V, Tamada JA, Klibanov AM, Langer R (1991) Kinetics of insulin aggregation in aqueous solutions upon agitation in the presence of hydrophobic surfaces. Proc Natl Acad Sci USA 88:9377–9381
8. Ferrão-Gonzales AD, Souto SO, Silva JL, Foguel D (2000) The preaggregated state of an amyloidogenic protein: hydrostatic pressure converts native transthyretin into the amyloidogenic state. Proc Natl Acad Sci USA 97:6445–6450
9. Bucciantini M, Giannoni E, Chiti F, Baroni F, Formigli L, Zurdo J, Taddei N, Ramponi G, Dobson CM, Stefani M (2002) Inherent toxicity of aggregates implies a common mechanism for misfolded disease. Nature 416:507–511
10. Nilsson MR (2004) Techniques to study amyloid fibril formation in vitro. Methods 34:151–160
11. Lakowicz JR (2006) Principles of fluorescence spectroscopy, 3rd edn. Kluwer Academic/Plenum, New York
12. Fluorescence Spectroscopy in Biology (2005) Hof M, Hutterer R, Fidler V (Eds.) Vol. 3, Springer, Berlin Heidelberg
13. Nilsson MR, Dobson CM (2003) In vitro characterization of lactoferrin aggregation and amyloid formation. Biochemistry 42:375–382
14. Sasahara K, Yagi H, Sakai M, Naiki M, Goto Y (2008) Amyloid nucleation triggered by agitation of β2-microglobulin under acidic and neutral pH conditions. Biochemistry 47:2650–2660

15. Jiménez JL, Nettleton EJ, Bouchard M, Robinson CV, Dobson CM, Saibil HR (2002) The protofilament structure of insulin amyloid fibrils. Proc Natl Acad Sci USA 99:9196–9201

16. Padrick SB, Miranker AD (2002) Islet amyloid: phase partitioning and secondary nucleation are central to the mechanism of fibrillogenesis. Biochemistry 41:4694–4703

17. Mukhopadhyay S, Nayak P, Udgaonkar JB, Krishnamoorthy G (2006) Characterization of amyloid fibril formation by mapping residue-specific fluorescence dynamics. J Mol Biol 358:935–942

18. Itzhaki LS, Evans PA, Dobson CM, Radford SE (1994) Tertiary interactions in the folding pathway of hen lysozyme: kinetic studies using fluorescent probes. Biochemistry 33:5212–5220

19. Rothwarf DM, Scheraga HA (1996) Role of non-native aromatic and hydrophobic interactions in the folding of hen egg white lysozyme. Biochemistry 35:13797–13807

20. Bachmann A, Segel D, Kiefhaber T (2002) Test for cooperativity in the early kinetic intermediate in lysozyme folding. Biophys Chem 96:141–151

21. Booth DR, Sunde M, Bellotti V, Robinson CV, Hutchinson WL, Fraser PE, Hawkins PN, Dobson CM, Radford SE, Blake CCF, Pepys MB (1997) Instability, unfolding and aggregation of human lysozyme variants underlying amyloid fibrillogenesis. Nature 385:787–793

22. Dumoulin M, Kumita JR, Dobson CM (2006) Normal and aberrant biological self-assembly: insights from studies of human lysozyme and its amyloidogenic variants. Acc Chem Res 39:603–610

23. Merlini G, Bellotti V (2005) Lysozyme: a paradigmatic molecule for the investigation of protein structure, function and misfolding. Clin Chim Acta 357:168–172

24. Frare E, Mossuto MF, de Laureto PP, Tolin S, Menzer L, Dumoulin M, Dobson CM, Fontana A (2009) Characterization of oligomeric species on the aggregation pathway of human lysozyme. J Mol Biol 387:17–27

25. Canet D, Sunde M, Last AM, Miranker A, Spencer A, Robinson CV, Dobson CM (1999) Mechanistic studies of the folding of human lysozyme and the origin of amyloidogenic behavior in its disease-related variants. Biochemistry 38:6419–6427

26. Frare E, de Laureto PP, Zurdo J, Dobson CM, Fontana A (2004) A highly amyloidogenic region of hen lysozyme. J Mol Biol 340:1153–1165

27. Morshedi D, Ebrahim-Habibi A, Moosavi-Movahedi AA, Nemat-Gorgani M (2010) Chemical modification of lysine residues in lysozyme may dramatically influence its amyloid fibrillation. Biochim Biophys Acta 1804:714–722

28. Malisauskas M, Ostman J, Darinskas A, Zamotin V, Liutkevicius E, Lundgren E, Morozova-Roche LA (2005) Does the cytotoxic effect of transient amyloid oligomers from common equine lysozyme in vitro imply innate amyloid toxicity? J Biol Chem 280:6269–6275

29. Gharibyan AL, Zamotin V, Yanamandra K, Moskaleva OS, Margulis BA, Kostanyan IA, Morozova-Roche LA (2007) Lysozyme amyloid oligomers and fibrils induce cellular death via different apoptotic/necrotic pathways. J Mol Biol 365:1337–1349

30. Holley M, Eginton C, Schaefer D, Brown LR (2008) Characterization of amyloidogenesis of hen egg lysozyme in concentrated ethanol solution. Biochem Biophys Res Commun 373:164–168

31. Moosavi-Movahedi AA, Pirzadeh P, Hashemnia S, Ahmadian S, Hemmateenejad B, Amani M, Saboury AA, Ahmad F, Shamsipur M, Hakimelahi GH, Tsai FY, Alijanvand HH, Yousefi R (2007) Fibril formation of lysozyme upon interaction with sodium dodecyl sulfate at pH 9.2. Colloids Surf B Biointerfaces 60:55–61

32. Kumar S, Ravi VK, Swaminathan R (2008) How do surfactants and DTT affect the size, dynamics, activity and growth of soluble lysozyme aggregates? Biochem J 415:275–288

33. Vernaglia BA, Huang J, Clark ED (2004) Guanidine hydrochloride can induce amyloid fibril formation from hen egg-white lysozyme. Biomacromolecules 5:1362–1370

34. Pertinhez TA, Bouchard M, Smith RAG, Dobson CM, Smith LJ (2002) Stimulation and inhibition of fibril formation by a peptide in the presence of different concentrations of SDS. FEBS Lett 529:193–197

35. Andersen KK, Oliveira CL, Larsen KL, Poulsen FM, Callisen TH, Westh P, Pedersen JS, Otzen D (2009) The role of decorated SDS micelles in sub-CMC protein denaturation and association. J Mol Biol 391:207–226

36. Stenstam A, Khan A, Wennerström H (2001) The lysozyme-dodecyl sulfate system. An example of protein-surfactant aggregation. Langmuir 17:7513–7520

37. Chatterjee A, Moulik SP, Majhib PR, Sanyal SK (2002) Studies on surfactant—biopolymer interaction. I. Microcalorimetric investigation on the interaction of cetyltrimethylammonium bromide (CTAB) and sodium dodecylsulfate (SDS) with gelatin (Gn), lysozyme (Lz) and deoxyribonucleic acid (DNA). Biophys Chem 98:313–327

38. Pirzadeh P, Moosavi-Movahedi AA, Hemmateenejad B, Ahmad F, Shamsipur M, Saboury AA (2006) Chemometric studies of lysozyme upon interaction with sodium dodecyl sulfate and β-cyclodextrin. Colloids Surf B Biointerfaces 52:31–38

39. Yamashita S, Nishimoto E, Szabo AG, Yamasaki N (1996) Steady-state and time-resolved fluorescence studies on the ligand-induced conformational change in an active lysozyme derivative, Kyn62-Lysozyme. Biochemistry 35:531–537

40. Chowdhury RP, Chatterji D (2007) Estimation of Förster's distance between two ends of Dps protein from mycobacteria: distance heterogeneity as a function of oligomerization and DNA binding. Biophys Chem 128:19–29

41. Semisotnov GV, Rodionova NA, Razgulyaev OI, Uversky VN, Gripas AF, Gilmanshin RI (1991) Study of the 'molten globule' intermediate state in protein folding by a hydrophobic fluorescent probe. Biopolymers 31:119–128

42. Lindgren M, Sörgjerd K, Hammarström P (2005) Detection and characterization of aggregates, prefibrillar amyloidogenic oligomers, and protofibrils using fluorescence spectroscopy. Biophys J 88:4200–4212

43. Fuguet E, Ráfols C, Rosés M, Bosch M (2005) Critical micelle concentration of surfactants in aqueous buffered and unbuffered systems. Anal Chim Acta 548:95–100

44. Wu LZ, Sheng YB, Xie JB, Wang W (2008) Photoexcitation of tryptophan groups induced reduction of disulfide bonds in hen egg white lysozyme. J Mol Struct 882:101–106

45. Frieden C (2007) Protein aggregation processes: in search of the mechanism. Protein Sci 16:2334–2344